J.Natn.Sci.Foundation Sri Lanka 2017 45 (2): 159-168
DOI: http://dx.doi.org/10.4038/jnsfsr.v45i2.8181

RESEARCH ARTICLE

Effect of T-shaped spur dike on flow separation in a 90° bend using SSIIM model

Mohammad Vaghefi*, Yaser Safarpoor and Seyed Shaker Hashemi
Department of Civil Engineering, Faculty of Engineering, Persian Gulf University, Shahid Mahini Street, P.O. Box 75169-13817, Bushehr, Iran.

Revised: 18 October 2016; Accepted: 08 December 2016

Abstract: Spur dikes are used widely as flow control structures in rivers. The main direction of the flow is changed by a spur dike, which is accompanied by formation of separation and reattachment zones around the spur dike. This study was focused on the effect of a submerged single T-shaped spur dike and the influence of the distance between non-submerged T-shaped spur dikes, in determining the separation and reattachment zones in a 90° bend using the SSIIM (sediment simulation in intakes with multi-block option) numerical model. The spur dike was installed at the middle of the outer bank in a movable-bed channel. It was observed that by increasing the submergence ratio, the length of separation and reattachment zones can be reduced, and by increasing the distance between two spur dikes the length of reattachment zone downstream of spur dikes can be increased. For all submergence ratios, from the bed level upwards to the crest level of the spur dike, the length of flow separation zone decreases, but the length of flow reattachment zone increases (dike crest level is equal to water depth level on the dike). By changing the dike submergence, the dimensions of the vortices around the dike can be changed due to variations in the flow separation and reattachment zones.

Keywords: Separation zone, SSIIM model, submergence, T- shaped spur dike.

INTRODUCTION

Spur dikes are usually used for two purposes; river training and erosion protection of river banks. Such dikes may be built as a single structure, namely, a single spur dike, or as a series of spur dikes along one or both banks of a river. The flow pattern in the vicinity of a single non-submerged spur dike can be divided into four main zones: main flow zone, return flow zone, separation streamline and reattachment point (Azinfar, 2010). Numerous studies have been conducted on the flow pattern and separation zone associated with spur dikes. The flow downstream of a spur dike is divided into three zones: main flow zone, wake zone and mixing zone. The reattachment zone is an area where the separated flows reattach the outer bank at downstream of the spur dike (Zhang & Nakagawa, 2008). The separation zone is an area upstream of the dike between the separated flow and dike axis. Figure 1 shows the separation length upstream of the dike. Vortices upstream and downstream of spur dikes are associated with the separation and reattachment zones. These vortices are the main cause of changes in topography of the channel bed. The length of reattachment zone is very important in choosing the location of structures in the river downstream.

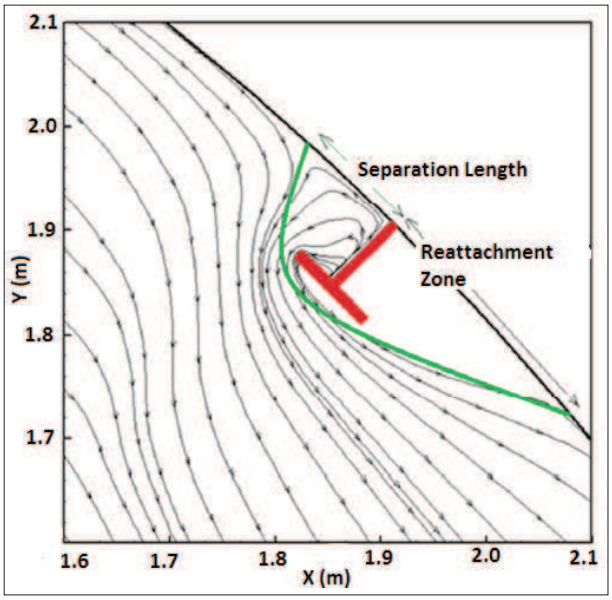

Figure 1: Separation and reattachment zones around spur dike

* Corresponding author (vaghefi@pgu.ac.ir)

Shukry (1950) studied the flow pattern in bends and presented a criterion to calculate the strength of the secondary flow. Ishii *et al.* (1983) reported that the shape of the separation region is hardly affected by the Froude number (Fr), and had dimensions of a length that ranged from 10 to 12 times the spur length. Chen and Ikeda (1997) have suggested the dimensionless length of reattachment zone based on the ratio of the length of dike (groin); and observed that the length of reattachment zone is almost constant and the reattachment point is located at a distance of about 14 times the length of the groin. The separation region has a length that could vary from 7 times (for relatively long groin) to 15 times the groin length. Yet, the relative width varies less and has a value that is slightly less than twice the groin length (Yossef, 2002). Ouillon and Dartus (1997) have reported that experiments have shown the length of reattachment zone to be 11.5 times the spur dike length while numerical studies have shown that it is 10.7 times the spur dike length. Elawady *et al*. (2001) studying bed scour around submerged spur dikes have concluded that local scour around submerged spur dikes is significantly affected by the overtopping ratio of the dike (water depth on the dike), and the opening ratio of the channel (the channel contraction).

The flow pattern near a single submerged spur dike is more complicated than that near a non-submerged spur dike. The three-dimensional flow in such a case has two types of vortices: vertical vortices and a vortex with intersecting axis. Tominga *et al.* (2001) have concluded that vortices with vertical axes lead to flow separation from the cape of the spur dike, whereas a vortex with an intersecting axis leads to flow separation from the crest of the spur dike. Ettema and Musto (2004) have conducted experiments in a channel with a rigid bed and constant width to determine the effect of a spur dike on the flow pattern and to determine the separation zones upstream and downstream of the dike. Uijttewaal (2005) observed the effect of geometry on the flow field around a spur dike and concluded that the ratio of length to width of the separation zone is related to the number and shape of the vortices in the return zone.

Attia and Elsaid (2006) studied three types of oriented groins with an angle of 60° defining the repelling groin type, which points towards the upstream direction or opposite to the flow direction, and an angle of 90° defining the straight groin or the groin perpendicular to the flow direction. An angle of 120° defines the attracting type groin pointing in the downstream direction or the flow direction. A straight groin of 90° orientation angle has the longest reattachment length. The contraction ratio is defined as the ratio of the groin length to channel width. All contraction ratios of the repelling type groins have longer reattachment lengths than the corresponding angles of attracting groins. The straight groins with 90° orientation give the lowest length for the separation points. It can be concluded that using the spur dike orientations, the contraction ratios should be adjusted according to the practical length needed in the channel for different purposes. Fazli *et al.* (2008) established a dike in different parts of the channel bend, and observed that with the increase of spur dike angle from the bend entry, the dimensions of flow separation upstream of spur dike increases and the dimensions of scour depth also increase with increasing length of the spur dike. Yazdi *et al.* (2010) by studying the flow pattern around a spur dike with a free surface, found that varying discharge has no significant effect on the reattachment length, but the length of the spur dike has a considerable effect on the dimensions of recirculation zone. A very complex 3 dimensional flow develops around the spur dike, with separation regions in front and behind the spur dike (Rodi, 2010). Abhari *et al*. (2010) studied the flow pattern at a 90° bend numerically and showed that the sediment simulation in intakes with multi-block option (version 1) (SSIIM-1) model could accurately simulate the flow pattern at a 90° bend. The studies of Vaghefi *et al*. (2014; 2015) have indicated that the SSIIM model (version 1) analyses the flow patterns and sediment at a 90° bend with a good approximation.

In view of these considerations, it is evident that the SSIIM model can be used for fluid dynamic computations at a river bend. No comprehensive studies have been carried out on the flow separation characteristics of T-shaped spur dikes. A T-shaped spur dike due to its special shape (the dike wing), has a different effect on the flow pattern than in the case of direct spur dikes. In the case of a T-shaped dike, an additional length of the channel is blocked by the dike wing. The ratios of dike submergence change during its operation. Therefore, in this study efforts have been made to study this effect. The case of installation of two spur dikes was also considered. In this study, the separation and reattachment zones around the T-shaped spur dike for two cases, namely, single and double spur dikes located at the outer bank at a 90° bend were considered.

METHODOLOGY

In two cases, the separation and reattachment zones have been investigated numerically. The two cases are, a single submerged spur dike at different submergence ratios (case 1), and the effects of spacing between two T-shaped spur dikes (case 2).

Experimental model set-up

The experiments were carried out at the Hydraulics Laboratory of Tarbiat Modares University, Iran, using a laboratory flume of 60 cm width and 70 cm height with a compound segment, which consisted of straight and bend route segments according to Figure 2. The length of the straight upstream route was 710 cm, which was connected to the straight downstream route of length 520 cm *via* a 90° bend with an external radius of 270 cm and an internal radius of 210 cm. A T-shaped spur dike was used in the experiment, and it consisted of two parts that are connected as shown in Figure 3(a). The length of the wing and web of the dike are equal to 9 cm. This spur dike was placed vertically (perpendicular to flow direction) at the middle of the outer bank and it was non-submerged during the experiment. The ratio of bend radius to width of the channel was 4. The Froude number of the flow at the bend entry was 0.34. The experiment was continued as long as the changes of bed topography became small. The duration of experiment was selected as 24 hrs during which, the change in bed topography was less than 2 mm at 4 consecutive hour periods. Depth of the flow was measured by a digital point gauge having an accuracy of ± 0.01 mm. The measurement of the bed topography was made by a laser bed profiler at different lateral sections. The flow measurement and components of 3-dimensional velocity were measured by the ADV-vectrino at several horizontal layers for different radial sections.

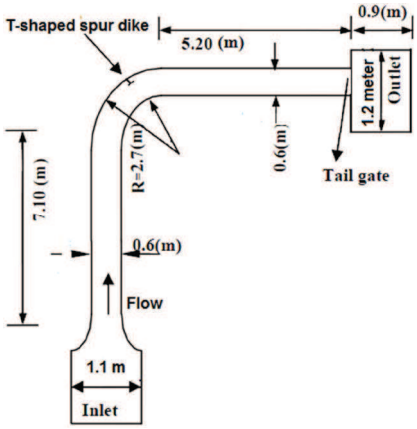

(a)

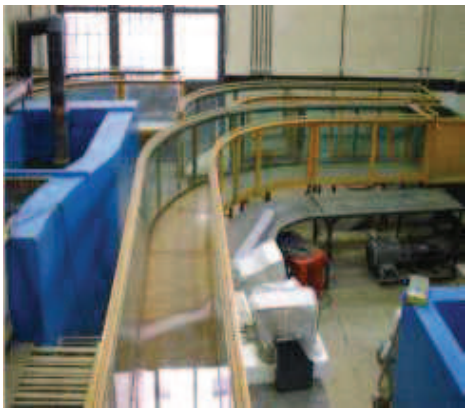

(b)

Figure 2: Experimental model set-up (a) plan and details; (b) photos of channels

Numerical model

The SSIIM numerical model solves the Navier-Stokes equations with the *k-epsilon* model on a three-dimensional general non-orthogonal grid. In SSIIM, the Navier-Stokes equations for turbulent flow in a general three-dimensional geometry are solved to obtain the water velocity. The Navier-Stokes equations for a flow that is non-compressible and with constant density can be expressed by equation (1).

$$\frac{\partial U_i}{\partial t} + U_j \frac{\partial U_i}{\partial x_i} = \frac{1}{\rho}\frac{\partial}{\partial x_i}\left(-P\delta_{ij} - \rho\overline{u_i u_j}\right) \quad ...(1)$$

where $x_i = x_1$, x_2 and x_3 are distances and $U_i = U_1$, U_2 and U_3 are the velocities in the three directions. P is the pressure, δ_{ij} is the Kronecker Delta that is equal to unity for i = j and zero otherwise. $\partial U_i / \partial t$ on the left side of the equation is the transient term and $U_j(\partial U_i / \partial x_i)$ is the convective term. $(\partial/\partial x_i)P\delta_{ij}$ on the right-hand side is the pressure term; $(\partial/\partial x_i)\rho u_i u_j$ is the Reynolds stress term and to evaluate this *k-epsilon* turbulence model is used. The semi-implicit method for pressure-linked equations (SIMPLE method) computes the pressure term (Olsen, 1999; 2000). In SSIIM-1 (version 1) a structured grid is used. In this study, the grid systems in the vertical, lateral and longitudinal directions had 26, 36 and 65 lines, respectively and the total number of cells was 60840. The grid system was checked using a finer mesh, where the number of gridlines was doubled in all directions. It was observed that under this condition the computational time of numerical analysis is too long and it was not suitable for practical purposes, while the results of the analysis are identical for two grid systems. The effective roughness was computed by van Rijn equation (van Rijn, 2007). Some of the limitations of the

programme are as follows: the programme is not made for the marine environment; kinematic viscosity of the fluid is equivalent to water at 20° C, which cannot be changed; the gridlines in the vertical direction have to be exactly vertical (Olsen, 2009).

Numerical model set-up

A straight T-shaped spur dike (perpendicular to the flow direction) was installed at a 90° channel bend with a movable bed in a mild curve (R/B = 4) as indicated in Figure 3. The walls of the channel were taken as rigid. The density of sediment particles was 2.35 g/cm^3. The initial water depth upstream of channel and at the start of bend was 11.6 cm. Uniform sediments with an average diameter of 1.28 mm were used and the discharge in the channel was measured at 25 Ls^{-1}. The standard deviation of the size of bed particles was 1.3. The studies were carried out under clear water conditions. In case 1, the spur dike was installed at the middle section of the channel bend on its outer bank, which has an angle of 45° with the bend entry as shown in Figure 3(b) named as first dike. In case 2, the second straight dike was installed at different distances relative to the first spur dike. The locations of the second dike are given in Table 1, where θ is the angle of each cross section relative to the bend entry at upstream as shown in Figure (3); S is the distance between two spur dikes; L is the spur dike length. For clarification purposes, an example of the gridding system at channel cross section (θ = 45°) with the submerged spur dike is shown in Figure 4.

Table 1: The locations of second dike in channel according to the first dike and spacing between dikes

Spacing between spur dikes	Second spur dike position
S = 2.5 L	θ = 49.9°
S = 3.5 L	θ = 51.8°
S = 5L	θ = 54.7°

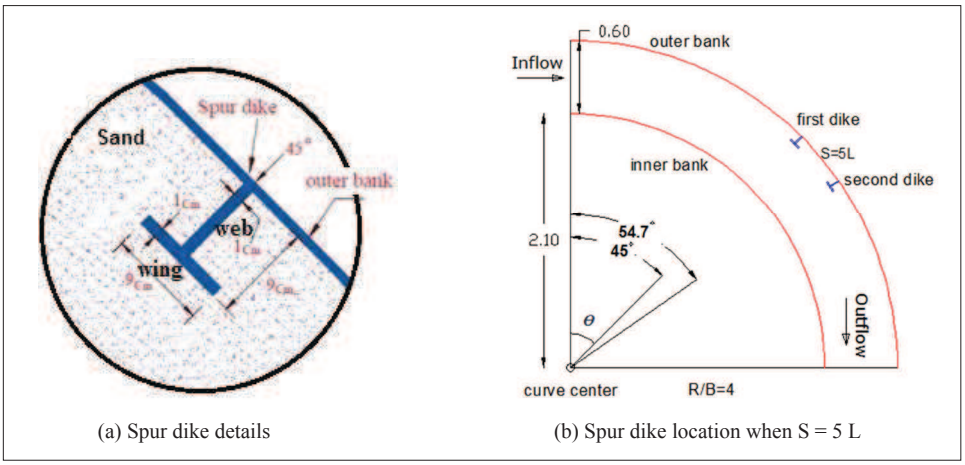

(a) Spur dike details (b) Spur dike location when S = 5 L

Figure 3: Channel bend and spur dike plans (a) dike details; (b) dike location

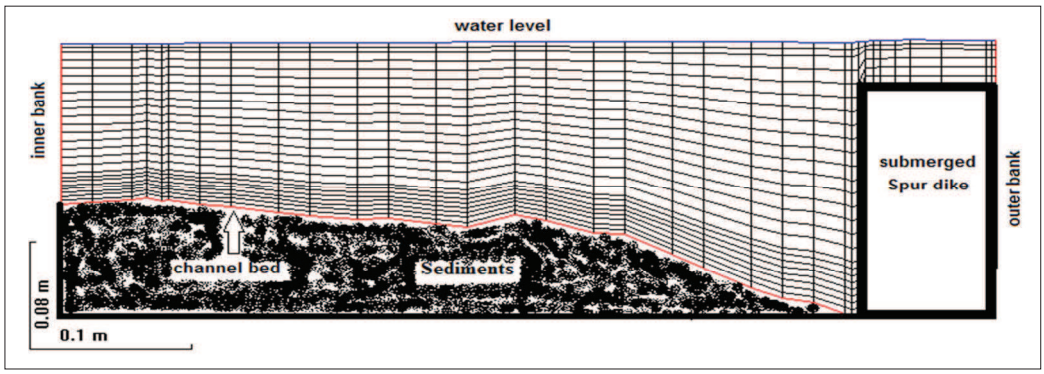

Figure 4: The gridding system at channel cross section (θ = 45°) with the submerged dike in outer bank

At first, the numerical model was calibrated with the experimental model results for non-submerged single spur dike. Then, using the calibrated numerical model, different cases of the submerged spur dike and the distance between two spur dikes were studied. The calibrated parameters are as follows: time step = 20 s; turbulence model (*k-epsilon)*; sediments fall velocity = 0.11 m/s; sediment transport equation; Shield's coefficient = 0.43; time of numerical run; bed and wall roughness were chosen as constants and the corresponding Strickler value is k_{st} = 64 $m^{1/3}$/s.

Boundary conditions

The discharge was introduced as the boundary condition at the entry of the computational domain. The gradient of all parameters were set to zero at the downstream boundary of the model. The flux passing the bed and walls was zero. The wall law of Schlichting (1979), as indicated in equation 2, was used for wall friction of the bend in all cases. On the water surface, zero gradient boundary conditions were used for the loss of turbulent kinetic energy, k, which was set to zero. Symmetrical boundary conditions were used for the water velocity, meaning that zero gradient boundary conditions were used for the velocities in the horizontal directions. The velocity in the vertical direction was calculated from the criteria of zero water flux across the water surface.

$$\frac{U}{U^*} = \frac{1}{k} ln\left(30\ y / k_s\right) \quad ...(2)$$

where U is the velocity, U^* is the shear velocity, k is a coefficient equal to 0.4, y is the distance from wall to the center of the cell, and k_s is wall roughness (Olsen, 2001; 2009).

Verification

The numerical model has been verified by experimental model results (Vaghefi *et al*., 2012). The comparison of the flow patterns, longitudinal velocities and bed profiles are shown in Figures 5, 6 and 7. The clear agreement between the numerical and experimental results indicate that the SSIIM model can be used for the investigation of flow in the vicinity of spur dikes and channel bend, and also could accurately simulate the separation zone at a 90° bend.

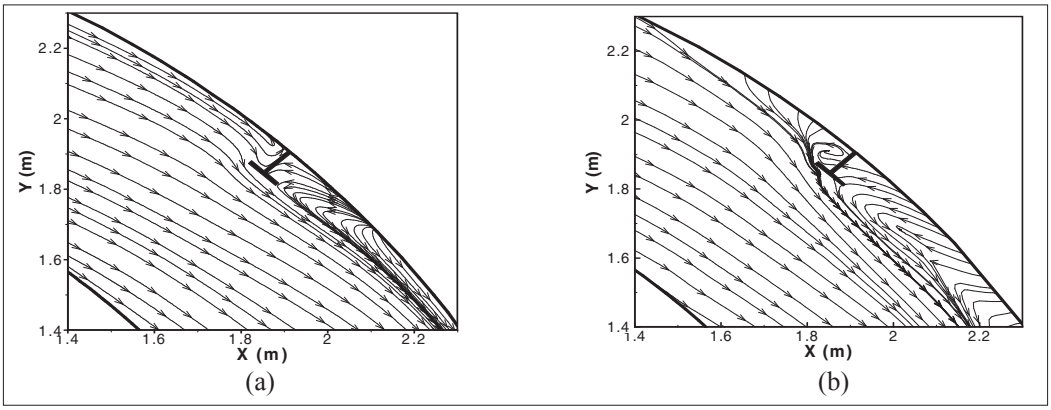

Figure 5: Flow pattern of water surface (a) numerical model; (b) laboratory model

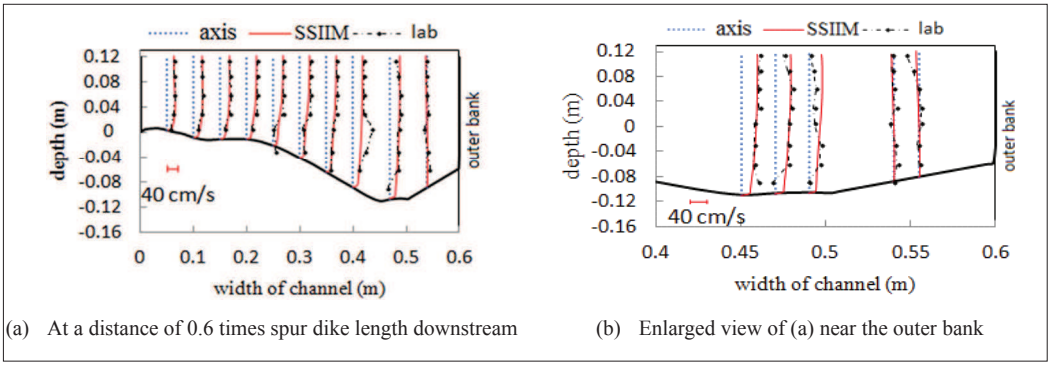

(a) At a distance of 0.6 times spur dike length downstream (b) Enlarged view of (a) near the outer bank

Figure 6: Longitudinal velocity in channel cross section in downstream of dike (a) total width of the channel; (b) part of channel width

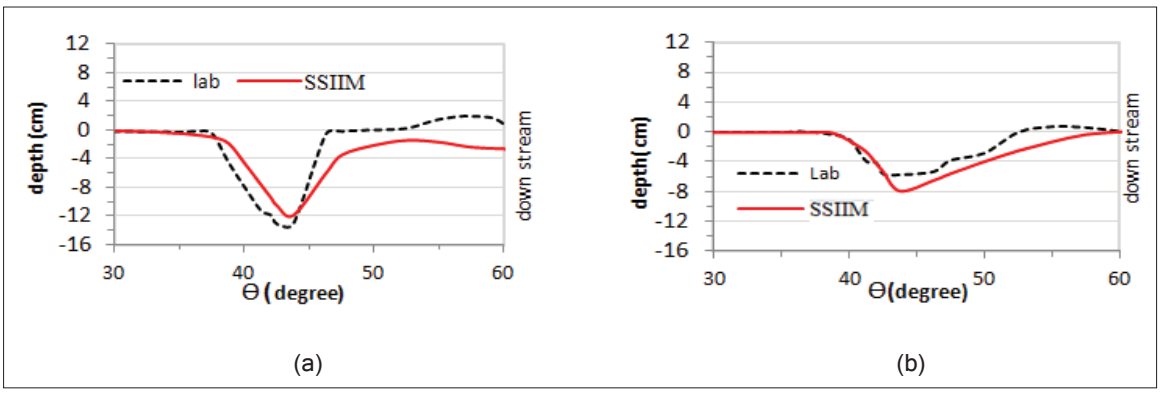

Figure 7: Longitudinal profile within (a) 5 cm; (b) 25 cm from the outer bank

RESULTS AND DISCUSSION

The velocities obtained by numerical modelling were converted into longitudinal and radial velocities using equations 3 and 4, and the flow pattern and velocity contours were plotted by appropriate computer software that used in post-processing simulation results such as Sigma plot and Tecplot 360 softwares.

$$U = U_r \sin\theta + V_\theta \cos\theta \quad ...(3)$$

$$V = U_r \cos\theta - V_\theta \sin\theta \quad ...(4)$$

where U and V are velocities in global axis, U_r is the radial velocity and V_θ is longitudinal velocity in the main direction. R is the radius of the bend. Velocity vectors are shown in Figure 8.

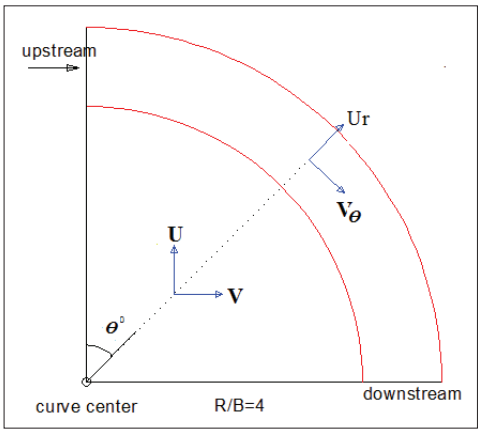

Figure 8: The longitudinal and radial velocities vectors in channel plan according to velocities in global axis

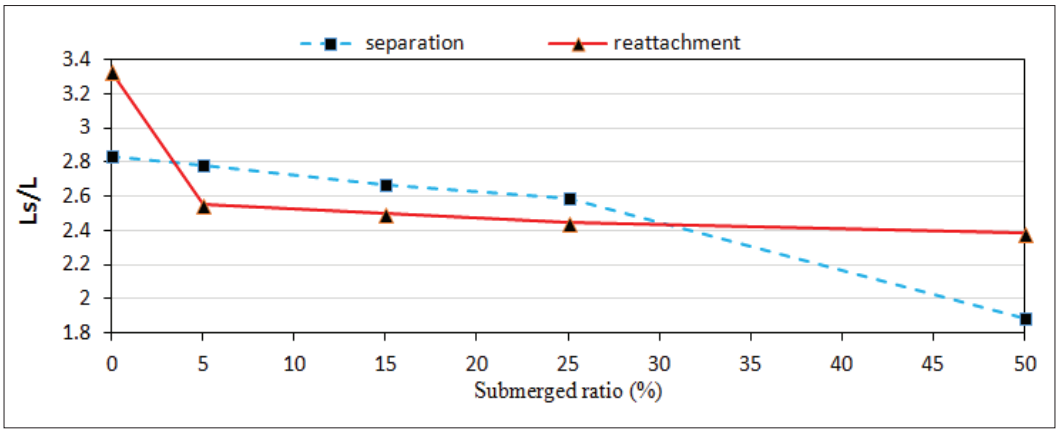

Figure 9: Length of separation and reattachment zones

Effect of submerged spur dike on separation and reattachment zones (case 1)

In this case, the effect of a single submerged spur dike at submergence ratios of 0, 5, 15, 25 and 50 % were investigated. The submergence ratio is defined as the ratio of h_1/H, where h_1 is the water depth on the dike and H is the total water depth in the channel. As indicated in Figure 9, the variation of the dimensionless lengths of separation and reattachment zones (L_s/L) with submergence ratio is presented, where L_s is the separation or reattachment length and L is the dike length. Based on the value of submergence ratio, it is evident that the flow separation zones related to a submergence ratio of 25 % to 50 % have changed significantly, indicating the lesser impact of spur dike on the flow pattern. The significant variation in the reattachment zone is also evidence for the submergence ratio from 0 % (non-submerged) to 5 %, and as in the submerged case, the flow passes over the crest level of spur dike and significantly decreases the length of reattachment zone. Therefore in general, it can be concluded that by increasing the submergence ratio, the length of separation and reattachment zones are reduced as indicated in Table 2.

Table 2: Reduction of the lengths of separation and reattachment zones due to submerged spur dikes

Increase in submergence ratio (%)	Reduction of the separation zone length (%)	Reduction of the reattachment zone length (%)	Increase in submergence ratio (%)	Reduction of the separation zone length (%)	Reduction of the reattachment zone length (%)
0 to 5	1.96	23.3	5 to 25	6.8	4.35
0 to 15	5.9	25	5 to 50	32	6.52
0 to 25	8.63	26.7	15 to 25	2.92	2.22
0 to 50	15.7	28.3	15 to 50	29.2	4.4
5 to 15	4	2.17	25 to 50	27	2.27

For all submergence ratios, from the bed level towards the crest level of spur dike (in submerged cases, spur dike crest level is equal to water depth level on the dike), the length of separation zone decreases but the length of reattachment zone increases. Due to the downward flow and longitudinal vortices upstream of spur dike, near the bed, part of the flow moves upstream and the velocity near the bed decreases compared to the velocity at higher layers. As a result, near the bed the length of the separation zone is higher than at water surface level.

Downstream of the spur dike near the outer bank, due to the formation of longitudinal vortices at the water surface, part of the flow moves upstream (toward the spur dike), whereas near the bed, it moves downstream to maintain the flow continuity.

Downstream of the spur dike at upper layers of the channel, the main stream encounters with the outer bank at a further distance compared to lower layers, thus the length of the reattachment zone increases by moving from the bed level towards the upper layers. As indicated in Table 3, by increasing the spur dike submergence ratio near the bed, the width of separation zone can be reduced as the length of the separation zone is also reduced.

Table 3: Reduction of the ratio of separation zone width to L at a level of 1.25 % of depth from the bed

Increase in submergence ratio (%)	Reduction of the dimensionless width of separation zone (%)	Increase in submergence ratio (%)	Reduction of the dimensionless width of separation zone (%)
0 to 5	3	5 to 25	18
0 to 15	9	5 to 50	46
0 to 25	21	15 to 25	13
0 to 50	47	15 to 50	42
5 to 15	6	25 to 50	34

Effect of spacing between two spur dikes on separation zone (case 2)

In this case, the effects of spacing between two T-shaped spur dikes on separation zone were investigated. The second spur dike was modelled at the distances of 2.5, 3.5 and 5 times of spur dike length from the first spur dike. In case 2, for all the spacings between the two spur dikes by moving from the bed layer towards upper layers, the length of separation zone decreases but the length of reattachment zone increases. By increasing the spacing between two spur dikes, no significant change occurred in the length of separation zone upstream of the first spur dike, but as expected the length of reattachment zone downstream of spur dikes increased as indicated in Table 4.

As indicated in Figures 10 and 11, velocity vectors can be seen at spur dikes field near the outer bank (at a distance of 0.8 % of channel width from outer bank) and near internal surface of the dike wing (at a distance of 12 % of channel width from outer bank) for single spur dike and when S = 2.5 L.

Table 4: Changes in length of reattachment zone on water level relative to single spur dike

Spacing between spur dikes	Ratio of the length of reattachment zone to the length of spur dike
S = 2.5 L	5.6
S = 3.5 L	6.65
S = 5 L	8.1

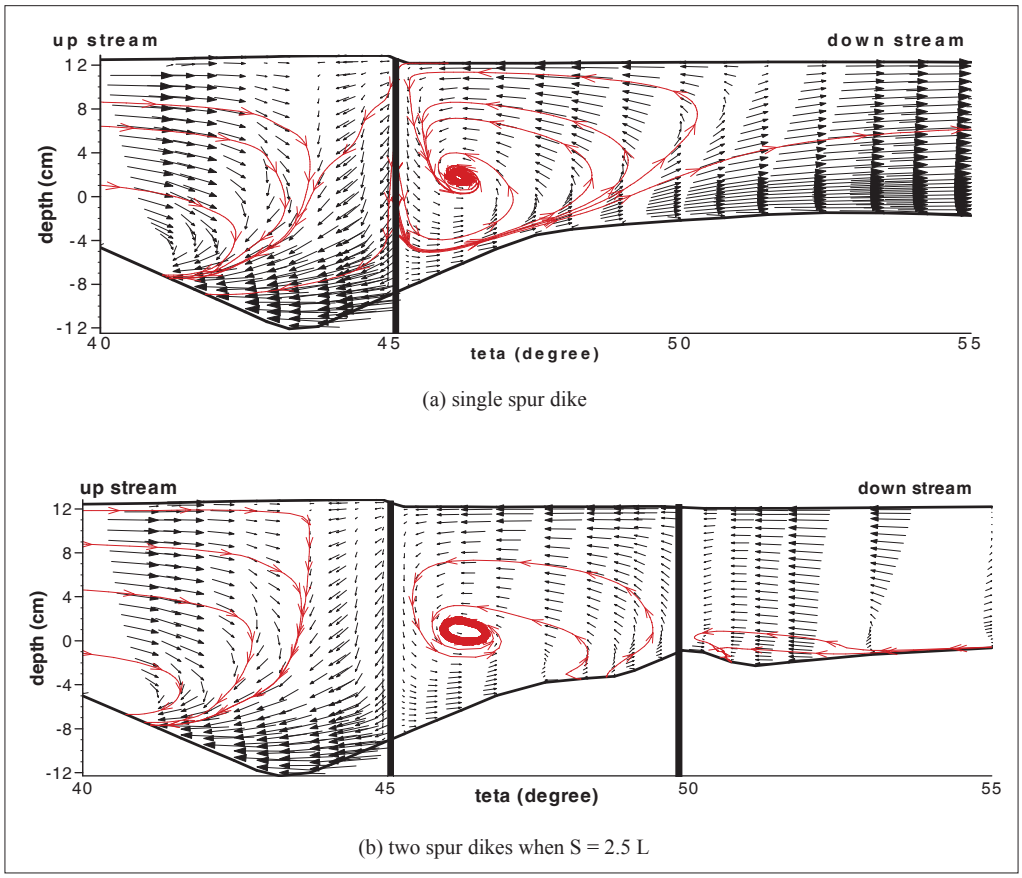

(a) single spur dike

(b) two spur dikes when S = 2.5 L

Figure 10: Vortices formed in two spur dikes field at distance of 0.8 % of channel width from outer bank

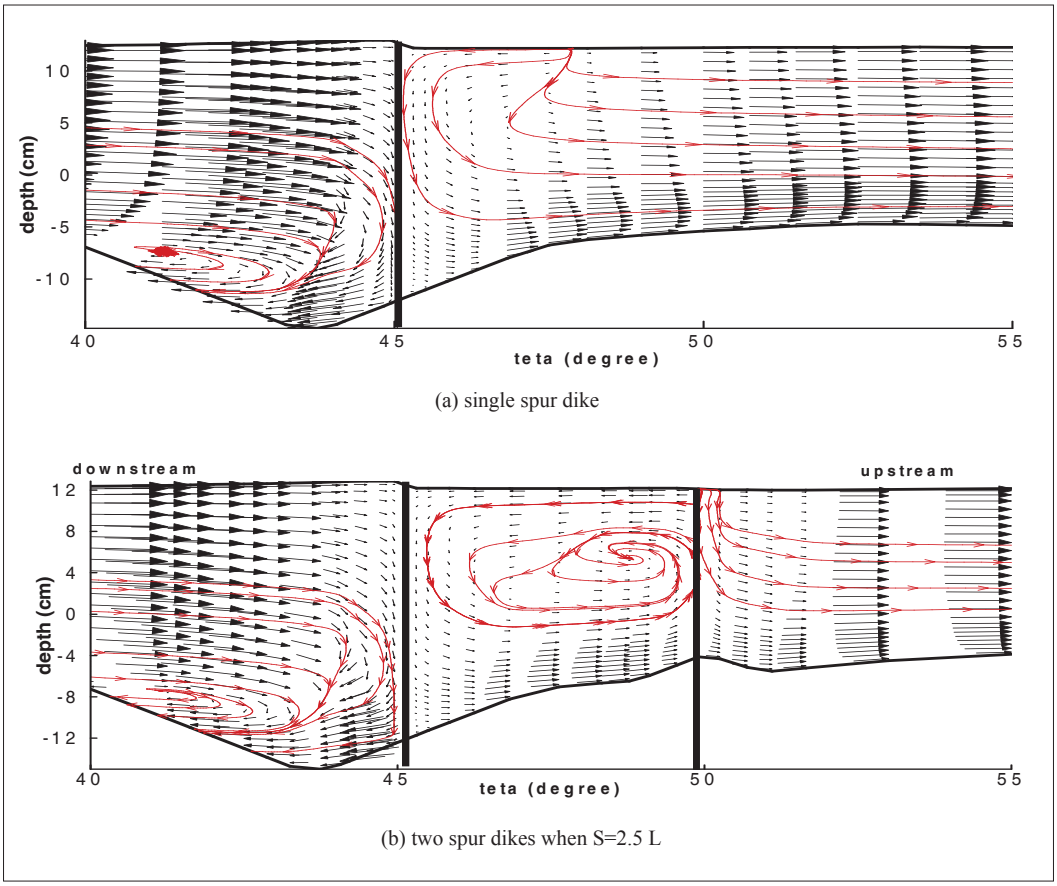

(a) single spur dike

(b) two spur dikes when S=2.5 L

Figure 11: Vortices formed in spur dikes field at a distance of 12 % of channel width from outer bank

CONCLUSION

The influence of spur dike submergence and spacing between two T- shaped spur dikes on the separation and reattachment zones were investigated in this study. Based on the results, it can be concluded that:

- With increasing spur dike submergence ratio, the width of separation zone near the bed decreases as the length of the separation zone is also reduced.
- For all submergence ratios considered from the bed layer towards upper layers, the length of flow separation zone decreases but the length of flow reattachment zone increases.
- With increasing the submergence ratio up to 50 %, the length of separation and reattachment zones decreases to 15.7 % and 28.3 %, respectively.
- Increasing the spacing between two spur dikes does not significantly change the length of separation zone upstream of the first spur dike, but increases the length of reattachment zone to 8.1 L relative to single spur dike downstream of spur dikes.
- Upstream of the first spur dike, the downward flow leads to the formation of a clockwise longitudinal vortex and the interaction of this vortex with the secondary flow leads to the formation of main scour hole.
- One important aspect in determining the distance between the spur dikes is the impact of separation and reattachment zones on channel upstream (or downstream) structures.
- By changing the dike submergence, the dimensions of vortices around the dike can be changed due to the variations in the flow separation and reattachment zones.

REFERENCES

1. Abhari M.N., Ghodsian M., Vaghefi M. & Panahpur N. (2010). Experimental and numerical simulation of flow in a 90° bend. *Journal of Flow Measurement and Instrumentation* **21**(3): 292 – 298.
2. Attia K.M. & Elsaid G. (2006). The hydraulic performance of oriented spur dike implementation in open channel. *Proceedings of the 10th International Water Technology Conference,* Alexandria, Egypt, pp. 162 – 171.
3. Azinfar H. (2010). Flow resistance and associated backwater effect due to spur dikes in open channels. *PhD thesis*, University of Saskatchewan, Saskatoon, Canada.
4. Chen F.Y. & Ikeda S. (1997). Horizontal separation in shallow open channels with spur dikes. *Journal of Hydro Science and Hydraulic Engineering* **15**(2): 15 – 30.
5. Elawady E., Michiue M. & Hinokidani O. (2001). Movable bed scour around submerged spur dikes. *Annual Journal of Hydraulic Engineering* **45**: 373 – 378. DOI: https://doi.org/10.2208/prohe.45.373
6. Ettema R. & Muste M. (2004). Scale effects in flume experiments on flow around a spur dike in flat bed channel. *Journal of Hydraulic Engineering* **130**(7): 635 – 646.
7. Fazli M., Ghodsian M. & Salehi Neyshabouri S.A.A. (2008). Scour and flow field around a spur dike in a 90° bend. *International Journal of Sediment Research* **23**(1): 56 – 68.
8. Ishii C., Asada H. & Kishi T. (1983). Shape of separation region formed behind a groyne of non-overflow type in rivers. *Proceedings of the* 20th IAHR Congress, 5 – 9 September, Moscow, Russia, pp. 405 - 412.
9. Olsen N.R.B. (1999). Computational fluid dynamics in hydraulic and sedimentation engineering. *Class Notes.* Department of Hydraulic and Environmental Engineering, Norwegian University of Science and Technology, Norway.
10. Olsen N.R.B. (2000). CFD algorithms for hydraulic Engineering. *Class Notes.* Department of Hydraulic and Environmental Engineering, Norwegian University of Science and Technology, Norway.
11. Olsen N.R.B. (2001). CFD modelling for hydraulic structures. *Class Notes* Department of Hydraulic and Environmental Engineering, Norwegian University of Science and Technology, Norway.
12. Olsen N.R.B. (2009). A three-dimensional numerical model for simulation of sediment movement in water intakes with multi-block option. *User's Manual.* Department of Hydraulic and Environmental Engineering, Norwegian University of Science and Technology, Norway.
13. Ouillon S. & Dartus D. (1997). Three-dimensional computation of flow around groyne. *Journal of Hydraulic Engineering* **123**(11): 962 – 970.
14. Rodi W. (2010). *Large Eddy Simulation of River Flows*. Institute for Hydromechanics, Karlsruhe Institute of Technology, Karlsruhe, Germany.
15. Schlichting H. (1979). *Boundary-Layer Theory*. McGraw-Hill, New York, USA.
16. Shukry A. (1950). Flow around bends in an open flume. *Transactions of the American Society of Civil Engineers* **115**(1): 751 – 779.
17. Tominaga A., Ijima K. & Nakano Y. (2001). Flow structures around submerged spur dikes with various relative height. In: Hydraulic Structures. *Proceedings of the 29th IAHR Congress*, Beijing, China, pp. 421 – 427.
18. Uijttewaal W.S.J. (2005). Effects of groins layout on the flow in groins fields: laboratory experiments. *Journal of Hydraulic Engineering* **131**(9): 782 – 791.
19. Vaghefi M., Ghodsian M. & Salehi Neyshabouri S.A.A. (2012). Experimental study on scour around a t-shaped spur dike in a channel bend. *Journal of Hydraulic Engineering* **138**(5): 471 – 474.
20. Vaghefi M., Safarpoor Y. & Hashemi S.S. (2014). Effect of T-shaped spur dike submergence ratio on the water surface profile in a 90° channel bends using SSIIM numerical model. *International Journal of Advanced Engineering Applications* **7**(4): 1 – 6.
21. Vaghefi M., Safarpoor Y. & Hashemi S.S. (2015). Effects of relative curvature on the scour pattern in a 90° bend with a T-shaped spur dike using a numerical method. *International Journal of River Basin Management* **13**(4): 501 – 514.
22. van Rijn L.C. (2007). Unified view of sediment transport by currents and waves-suspended transport. *Journal of Hydraulic Engineering* **133**(6): 668 – 689.
23. Yazdi J., Sarkardeh H., Azamathulla H.M. & Ghani A.A. (2010). 3-D simulation of flow around a single spur dike with free-surface flow. *International Journal of River Basin Management* **8**(1): 55 – 62. DOI: https://doi.org/10.1080/15715121003715107
24. Yossef M.F.M. (2002). *The Effect of Groynes on Rivers.* Section of Hydraulic Engineering, Delft University of Technology, The Netherlands.
25. Zhang H. & Nakagawa H. (2008). Scour around spur dike: resent advances and future researches. *Annuals of Disaster Prevention Research Institute*, *Kyoto University* **51**: 633 – 652.